

Evaluation of the H-point standard additions method (HPSAM) and the generalized H-point standard additions method (GHPSAM) for the UV-analysis of two-component mixtures

E. Hund, D.L. Massart, J. Smeyers-Verbeke *

ChemoAC, Pharmaceutical Institute, Vrije Universiteit Brussel, Laarbeeklaan 103, B-1090 Brussels, Belgium

Received 20 August 1998; received in revised form 10 December 1998; accepted 1 January 1999

Abstract

The H-point standard additions method (HPSAM) and two versions of the generalized H-point standard additions method (GHPSAM) are evaluated for the UV-analysis of two-component mixtures. Synthetic mixtures of anhydrous caffeine and phenazone as well as of atovaquone and proguanil hydrochloride were used. Furthermore, the method was applied to pharmaceutical formulations that contain these compounds as active drug substances. This paper shows both the difficulties that are related to the methods and the conditions by which acceptable results can be obtained. © 1999 Elsevier Science B.V. All rights reserved.

Keywords: H-point; Standard additions method; Analyte and interferent concentration; Binary mixtures; UV analysis

1. Introduction

The H-point standard additions method (HPSAM) was introduced as a modification of the standard additions method [1]. It was presented as an analysis method that permits determination of the concentration of the analyte free from both proportional and constant errors in the presence of a known interferent. It requires the spectrum of

the interferent to be known, as it is based on measurements at two wavelengths for which the interferent shows the same absorbance. Moreover, the HPSAM also allows calculation of the concentration of this interferent free from proportional error. The calculated interferent concentration will also be free from constant error if there is no additional constant error [2]. Very accurate results are reported even for extensively overlapping spectra in UV–visible spectrophotometry [3]. The method has also been adapted for resolving ternary mixtures [4].

As a further modification, the so-called generalized H-point standard additions method (GHP-

* Corresponding author. Tel.: +32-2-477-4737; fax: +32-2-477-4735.

E-mail address: asmeyers@fabi.vub.ac.be (J.Smeyers-Verbeke)

SAM) was presented [5] and recently an improvement of the method has been proposed [6]. In contrast to the HPSAM, the GHPSAM does not require knowledge of the spectrum of the interferent(s), but also allows determination of the concentration of the analyte free from both proportional and constant error. Some other methods that are frequently used in the analysis of binary and multi-component mixtures require the spectra of all the compounds to be known. GHPSAM seems to offer a useful alternative for the analysis of a known compound (the analyte) in an unknown matrix.

In the first publications, the HPSAM was applied to UV–visible spectrophotometry [1,3]. Later, it was also extended to liquid chromatography with diode array detection [7] and spectrofluorimetry [8].

The aim of the present work is to evaluate both methods for the UV analysis of pharmaceutical formulations containing two active substances. Synthetic mixtures of anhydrous caffeine and phenazone and of atovaquone and proguanil hydrochloride were used. Mixtures were prepared in which for caffeine/phenazone, caffeine was either considered as the analyte (and phenazone the interferent) or as the interferent (and phenazone the analyte). Similarly for proguanil hydrochloride/atovaquone, proguanil hydrochloride was either the analyte (and atovaquone the interferent) or the interferent (and atovaquone the analyte). Different ratios of analyte/interferent were considered for the evaluation. Furthermore, pharmaceutical formulations were included in the evaluation: caffeine monohydrate and phenazone are the active drug substances of Parmentier; Malarone contains atovaquone and proguanil hydrochloride.

2. Theory

An overview of the theoretical background of the H-point standard additions method (HPSAM) and the generalized H-point standard additions method (GHPSAM) is given in Appendix A.

3. Experimental

3.1. Equipment

The measurements were performed with a Shimadzu UV-2101 PC double-beam spectrophotometer, equipped with 1-cm pathlength quartz cells. The slit-width was 1.0 nm, all spectra were recorded with a scan speed of 42 nm/min at 0.1-nm intervals. For caffeine and phenazone, the spectra were recorded in the wavelength range 215–295 nm, whereas for atovaquone and proguanil the measurements were taken between 230 and 300 nm.

The computation routines were written using Matlab 4.0 (Math Works, Natick, MA).

3.2. Materials

Parmentier powders are commercially available. Phenazone (BF V) was obtained from Hoechst (Frankfurt/Main, Germany). Analytical grade anhydrous caffeine (Merck, Darmstadt, Germany) and analytical grade methanol (BDH, Poole, UK) were used. Atovaquone, proguanil hydrochloride and Malarone tablets were obtained from GlaxoWellcome (Dartford, UK).

3.3. Procedures

3.3.1. Synthetic mixtures

Mixtures containing the analyte and the interferent in different ratios were prepared. The composition of the different mixtures is shown in Table 1. For each mixture, solutions containing the same concentration of the interferent and increasing concentrations of the analyte were prepared to apply both the HPSAM and the GHPSAM. For all the measurements, six replicate solutions were prepared. The concentration range of analyte added as well as the number of additions made are also shown in Table 1.

3.3.2. Pharmaceutical formulations

3.3.2.1. *Parmentier*. Parmentier is a powder. The label specifies that each unit contains 200 mg caffeine monohydrate and 400 mg phenazone. Six

individual units of Parmentier were each dissolved independently in 100 ml methanol. The precipitate was separated by centrifugation. Each solution was diluted 500 times. Therefore, the solutions contain theoretically 18.85 and 42.51 $\mu\text{mol/l}$ of caffeine and phenazone, respectively. For the determination of phenazone, the concentration added for the addition methods varied from 0 to 59.81 $\mu\text{mol/l}$ ($n = 7$) and for caffeine from 0 to 58.61 $\mu\text{mol/l}$ ($n = 7$).

3.3.2.2. Malarone. Malarone tablets contain 250 mg of atovaquone and 100 mg of proguanil hydrochloride. From a powdered tablet, ± 200 mg was exactly weighted and dissolved in 200 ml 40% methanolic 0.1 M NaOH. After the separation of the insoluble compounds by centrifugation, the solution was diluted 10 times with an aqueous 0.1 M NaOH solution. This solution was further diluted 10 times with 4% methanolic 0.1 M NaOH. Therefore, the solution contains theoretically ± 14 and ± 7 $\mu\text{mol/l}$ of atovaquone and proguanil, respectively. Six solutions were independently prepared in that way from six individual tablets. For the analysis of the tablets, the concentration added for the addition methods varied from 0 to 16.55 $\mu\text{mol/l}$ ($n = 6$) for atovaquone and for proguanil hydrochloride from 0 to 41.14 $\mu\text{mol/l}$ ($n = 6$).

For the synthetic mixtures as well as for the pharmaceutical formulations, calibration lines were measured after every second addition line

both for the analyte and the interferent. They were used for the calculation of the concentration of the interferent in the HPSAM, and of the molar absorption coefficients required in the λ_{max} -method as well as for the calculation of the second derivatives of the molar absorption coefficients of the analyte in the GHPSAM.

4. Results and discussion

4.1. HPSAM

4.1.1. Mixtures of caffeine and phenazone

The mixtures containing caffeine and phenazone in different ratios were prepared in methanol. As can be seen from the spectra (Fig. 1a,b), there are several pairs of wavelengths that fulfill the requirement for the application of the HPSAM. Some of these wavelength pairs selected for the evaluation are shown in Fig. 1a,b.

The results for phenazone considered as the analyte in the synthetic mixtures are shown in Tables 2 and 3. The best results for the analyte in terms of precision and accuracy are generally obtained for the wavelength pair 290.0/244.5 nm that leads to the largest difference between the slopes of the standard addition lines ($M(\lambda_1) - M(\lambda_2)$). At this optimal wavelength pair, accuracy and precision are comparable to that of the λ_{max} -method, even if the contribution of the interferent in the spectrum of the mixture is larger than for

Table 1
Composition of the synthetic mixtures

Mixture	Analyte ($\mu\text{mol/l}$)	Interferent ($\mu\text{mol/l}$)	Added analyte, concentration range ($\mu\text{mol/l}$)	Number of additions
	Phenazone	Caffeine		
1	8.48	16.58	0–50.88	6
2	42.72	20.93	0–29.90	7
	Caffeine	Phenazone		
3	16.58	16.96	0–58.03	6
4	20.93	42.72	0–28.30	7
	Atovaquone	Proguanil-HCl		
5	13.71	6.86	0–16.55	6
	Proguanil-HCl	Atovaquone		
6	13.71	5.52	0–20.57	6
7	6.86	13.71	0–41.14	6

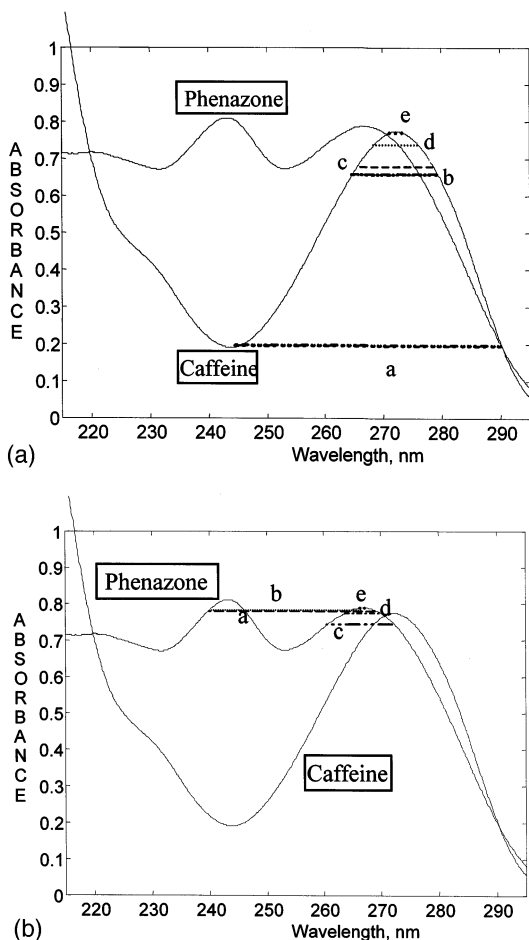


Fig. 1. (a) Absorption spectra of caffeine (82.9 $\mu\text{mol/l}$) and phenazone (84.8 $\mu\text{mol/l}$). Selection of wavelength pairs for caffeine as the interferent: a) 244.5/290.0 nm; b) 264.5/279.2 nm; c) 265.4/278.4 nm; d) 268.2/275.9 nm; e) 270.9/273.3 nm. (b) Absorption spectra of caffeine (82.9 $\mu\text{mol/l}$) and phenazone (84.8 $\mu\text{mol/l}$). Selection of wavelength pairs for phenazone as the interferent: a) 239.8/269.0 nm; b) 240.4/266.7 nm; c) 260.4/272.0 nm; d) 263.6/269.7 nm; e) 266.1/267.1 nm.

the analyte (Table 2). The results for the interferent (caffeine) determined from the absorbance at the H-point are considerably less precise than those obtained by the λ_{max} -method. They are also less accurate in mixture 2 (Table 3) in which the interferent (caffeine) contributes less to the spectrum of the mixture than the analyte. Table 4 shows the results for phenazone considered as the analyte in the analysis of the formulation Parmen-

tier. As an outlier was detected by means of a Dixon test [9], they are based on five replicates only. The wavelength pair resulting in the largest difference between the slopes of the standard addition lines (290.0/244.5 nm) again leads to a result similar to that of the λ_{max} -method. It has already been shown earlier that the latter method yields good results for the analysis of Parmentier [10]. The fact that the results of the wavelength pairs 279.2/264.5, 278.4/265.4 and 275.9/268.2 nm show a lower deviation from the theoretical value, is not a guarantee for a better accuracy at these wavelength pairs since the exact concentration of phenazone (and caffeine) in the formulation is not known. As with the synthetic mixtures, the results of caffeine (the interferent) based on the absorbance at the H-point show poorer precision than those obtained from the λ_{max} -method.

The results for caffeine considered as the analyte in the synthetic mixtures are shown in Tables 5 and 6. The wavelength pairs with the largest difference between the slopes of the standard addition lines ($M(\lambda_1) - M(\lambda_2)$), 269.0/239.8 and 266.7/240.4 nm, again lead to the best results both in terms of precision and accuracy. They are comparable to the results obtained for the λ_{max} -method. The concentrations of phenazone (the interferent) obtained from the absorbance at the H-point for these two wavelength pairs are also very similar to the results of the λ_{max} -method. Notice that in mixtures 3 (Table 5) and 4, which are simulations of Parmentier (Table 6), the concentration of phenazone is comparable (mixture 3) or larger (mixture 4), respectively, than that of the analyte. The results for caffeine considered as the analyte in the analysis of the Parmentier powders are given in Table 7. They are also based on five replicates only. For phenazone as the interferent, the wavelength pairs with the largest difference between the slopes of the standard addition lines show the same results as the λ_{max} -method. Precision and accuracy are comparable both for the concentration of the analyte (caffeine) and the concentration of the interferent (phenazone) obtained from the absorbance at the H-point.

4.1.2. Mixtures of atovaquone and proguanil hydrochloride

The mixtures of atovaquone and proguanil hydrochloride were prepared in 4% methanolic 0.1

M NaOH. Fig. 2a shows the absorption spectra of both components. The wavelength pairs for atovaquone and proguanil are relatively easy to select, but the useful wavelength range for proguanil as the interferent is not very large. The

Table 2
Results for mixture 1 from additions of phenazone^a

λ_1/nm ($\bar{M} \pm s_M$)*	λ_2/nm ($\bar{M} \pm s_M$)*	Phenazone found (C_H)		Caffeine found (from A_H)	
		$\mu\text{mol/l}$	%	$\mu\text{mol/l}$	%
290.0 (2428 \pm 41)	244.5 (9576 \pm 124)	8.38 \pm 0.14	98.8 \pm 1.7	17.21 \pm 0.80	103.8 \pm 4.8
279.2 (6817 \pm 74)	264.5 (9267 \pm 107)	7.46 \pm 0.22	87.9 \pm 2.6	18.32 \pm 0.42	110.5 \pm 2.5
278.4 (7113 \pm 81)	265.4 (9331 \pm 113)	7.25 \pm 0.25	85.5 \pm 2.9	18.53 \pm 0.47	111.7 \pm 2.8
275.9 (7964 \pm 90)	268.2 (9357 \pm 112)	7.16 \pm 0.21	84.4 \pm 2.5	18.43 \pm 0.34	111.2 \pm 2.1
273.3 (8657 \pm 106)	270.9 (9103 \pm 108)	6.14 \pm 0.45	72.5 \pm 5.3	19.37 \pm 0.71	116.8 \pm 4.3
λ_{max} : 242.8/272.2 nm		8.58 \pm 0.28	101.2 \pm 3.3	17.23 \pm 0.24	103.9 \pm 1.4

^a Phenazone (analyte): 8.48 $\mu\text{mol/l}$; caffeine (interferent): 16.58 $\mu\text{mol/l}$.

* \bar{M} , mean slope of the addition line; s_M , standard deviation of the slope.

Table 3
Results for mixture 2 from additions of phenazone^a

λ_1/nm ($\bar{M} \pm s_M$)*	λ_2/nm ($\bar{M} \pm s_M$)*	Phenazone found (C_H)		Caffeine found (from A_H)	
		$\mu\text{mol/l}$	%	$\mu\text{mol/l}$	%
290.0 (2367 \pm 34)	244.5 (9338 \pm 82)	43.27 \pm 0.39	101.3 \pm 0.9	22.78 \pm 1.09	108.8 \pm 5.2
279.2 (6652 \pm 61)	264.5 (9093 \pm 83)	40.99 \pm 0.61	95.9 \pm 1.4	23.90 \pm 0.55	114.2 \pm 2.6
278.4 (6944 \pm 74)	265.4 (9175 \pm 74)	40.45 \pm 0.35	94.7 \pm 0.8	24.35 \pm 0.47	116.3 \pm 2.2
275.9 (7778 \pm 86)	268.2 (9198 \pm 79)	39.18 \pm 0.83	91.7 \pm 1.9	25.33 \pm 0.89	121.0 \pm 4.3
273.3 (8510 \pm 84)	270.9 (8943 \pm 87)	40.65 \pm 1.65	95.2 \pm 3.9	23.59 \pm 1.49	112.7 \pm 7.1
λ_{max} : 242.8/272.2 nm		43.00 \pm 0.24	100.7 \pm 0.6	21.24 \pm 0.06	101.5 \pm 0.3

^a Phenazone (analyte): 42.72 $\mu\text{mol/l}$; caffeine (interferent): 20.93 $\mu\text{mol/l}$.

* \bar{M} , mean slope of the addition line; s_M , standard deviation of the slope.

Table 4
Results from additions of phenazone to Parmentier^a

λ_1/nm ($\bar{M} \pm s_M$)*	λ_2/nm ($\bar{M} \pm s_M$)*	Phenazone found (C_H)		Caffeine monohydrate found (from A_H)	
		mg/unit	%	mg/unit	%
290.0 (2353 \pm 6)	244.5 (9457 \pm 26)	413.4 \pm 6.4	103.4 \pm 1.6	213.1 \pm 7.1	106.6 \pm 3.6
279.2 (6723 \pm 5)	264.5 (9180 \pm 24)	403.4 \pm 5.5	100.9 \pm 1.4	210.5 \pm 7.6	105.2 \pm 3.8
278.4 (7028 \pm 6)	265.4 (9243 \pm 22)	404.5 \pm 5.6	101.1 \pm 1.4	208.8 \pm 5.7	104.4 \pm 2.9
275.9 (7859 \pm 7)	268.2 (9259 \pm 18)	403.6 \pm 4.1	100.9 \pm 1.0	208.0 \pm 7.2	104.0 \pm 3.6
273.3 (8557 \pm 10)	270.9 (9002 \pm 11)	381.0 \pm 13.4	95.2 \pm 3.4	231.1 \pm 13.5	115.5 \pm 6.8
λ_{max} : 242.8/272.2 nm		417.4 \pm 5.8	104.4 \pm 1.5	192.0 \pm 3.8	96.0 \pm 1.9

^a Phenazone (analyte): 400 mg/unit; caffeine monohydrate (interferent): 200 mg/unit.

* \bar{M} , mean slope of the addition line; s_M , standard deviation of the slope.

Table 5
Results for mixture 3 from additions of caffeine^a

$\lambda_1/\text{nm} (\bar{M} \pm s_M)^*$	$\lambda_2/\text{nm} (\bar{M} \pm s_M)^*$	Caffeine found (C_H)		Phenazone found (from A_H)	
		$\mu\text{mol/l}$	%	$\mu\text{mol/l}$	%
269.0 (8943 \pm 101)	239.8 (2589 \pm 91)	16.52 \pm 0.20	99.7 \pm 1.2	18.09 \pm 0.56	106.7 \pm 3.3
266.7 (8437 \pm 97)	240.4 (2508 \pm 93)	16.41 \pm 0.19	99.0 \pm 1.1	18.06 \pm 0.57	106.5 \pm 3.4
272.0 (9251 \pm 94)	260.4 (6414 \pm 85)	17.62 \pm 0.32	106.3 \pm 1.9	17.00 \pm 0.51	100.3 \pm 3.0
269.7 (9054 \pm 100)	263.6 (7505 \pm 90)	17.96 \pm 0.42	108.3 \pm 2.5	16.61 \pm 0.42	97.9 \pm 2.5
267.1 (8536 \pm 94)	266.1 (8273 \pm 95)	17.25 \pm 1.82	104.0 \pm 11	17.17 \pm 1.43	101.3 \pm 8.4
λ_{max} : 242.8/272.2 nm		16.56 \pm 0.11	99.9 \pm 0.7	17.86 \pm 0.40	105.3 \pm 2.4

^a Caffeine (analyte): 16.58 $\mu\text{mol/l}$; phenazone (interferent): 16.96 $\mu\text{mol/l}$.

* \bar{M} , mean slope of the addition line; s_M , standard deviation of the slope.

Table 6
Results for mixture 4 from additions of caffeine^a

$\lambda_1/\text{nm} (\bar{M} \pm s_M)^*$	$\lambda_2/\text{nm} (\bar{M} \pm s_M)^*$	Caffeine found (C_H)		Phenazone found (from A_H)	
		$\mu\text{mol/l}$	%	$\mu\text{mol/l}$	%
269.0 (9126 \pm 117)	239.8 (2696 \pm 119)	20.92 \pm 0.24	99.9 \pm 1.1	43.24 \pm 0.56	101.2 \pm 1.3
266.7 (8593 \pm 108)	240.4 (2611 \pm 111)	20.98 \pm 0.20	100.2 \pm 1.0	43.18 \pm 0.52	101.1 \pm 1.2
272.0 (9421 \pm 99)	260.4 (6483 \pm 110)	21.85 \pm 0.40	104.4 \pm 1.9	42.60 \pm 0.64	99.7 \pm 1.5
269.7 (9238 \pm 110)	263.6 (7626 \pm 113)	21.80 \pm 0.45	104.1 \pm 2.1	42.43 \pm 0.63	99.3 \pm 1.5
267.1 (8695 \pm 105)	266.1 (8424 \pm 109)	23.34 \pm 1.90	111.5 \pm 9.1	40.91 \pm 1.64	95.8 \pm 3.8
λ_{max} : 242.8/272.2 nm		21.13 \pm 0.19	100.9 \pm 0.9	43.48 \pm 0.24	101.8 \pm 0.6

^a Caffeine (analyte): 20.93 $\mu\text{mol/l}$; phenazone (interferent): 42.72 $\mu\text{mol/l}$.

* \bar{M} , mean slope of the addition line; s_M , standard deviation of the slope.

Table 7
Results from additions of caffeine to Parmentier^a

$\lambda_1/\text{nm} (\bar{M} \pm s_M)^*$	$\lambda_2/\text{nm} (\bar{M} \pm s_M)^*$	Caffeine monohydrate found (C_H)		Phenazone found (from A_H)	
		mg/unit	%	mg/unit	%
269.0 (9006 \pm 13)	239.8 (2642 \pm 11)	195.1 \pm 4.7	97.6 \pm 2.4	414.4 \pm 4.8	103.6 \pm 1.2
266.7 (8493 \pm 14)	240.4 (2554 \pm 14)	194.9 \pm 5.1	97.5 \pm 2.6	414.2 \pm 4.9	103.6 \pm 1.2
272.0 (9311 \pm 16)	260.4 (6465 \pm 13)	212.3 \pm 5.7	106.1 \pm 2.9	402.0 \pm 3.7	100.5 \pm 0.9
269.7 (9119 \pm 15)	263.6 (7559 \pm 20)	206.3 \pm 4.5	103.1 \pm 2.3	405.0 \pm 4.7	101.3 \pm 1.2
267.1 (8594 \pm 13)	266.1 (8332 \pm 18)	225.2 \pm 12.7	112.6 \pm 6.4	389.1 \pm 8.0	97.3 \pm 2.0
λ_{max} : 242.8/272.2 nm		192.5 \pm 4.0	96.3 \pm 2.0	413.8 \pm 4.8	103.5 \pm 1.2

^a Caffeine monohydrate (analyte): 200 mg/unit; phenazone (interferent): 400 mg/unit.

* \bar{M} , mean slope of the addition line; s_M , standard deviation of the slope.

wavelength pairs selected for the evaluation of the method for this pair of substances are indicated in Fig. 2b,c.

The results for atovaquone considered as the analyte are shown in Table 8. If only accuracy is

considered, all the wavelength pairs selected lead to comparable results of $\pm 95\%$. Notice however the high standard deviations of the slopes of the addition lines at the wavelengths lower than 240 nm: the lower this wavelength, the poorer the

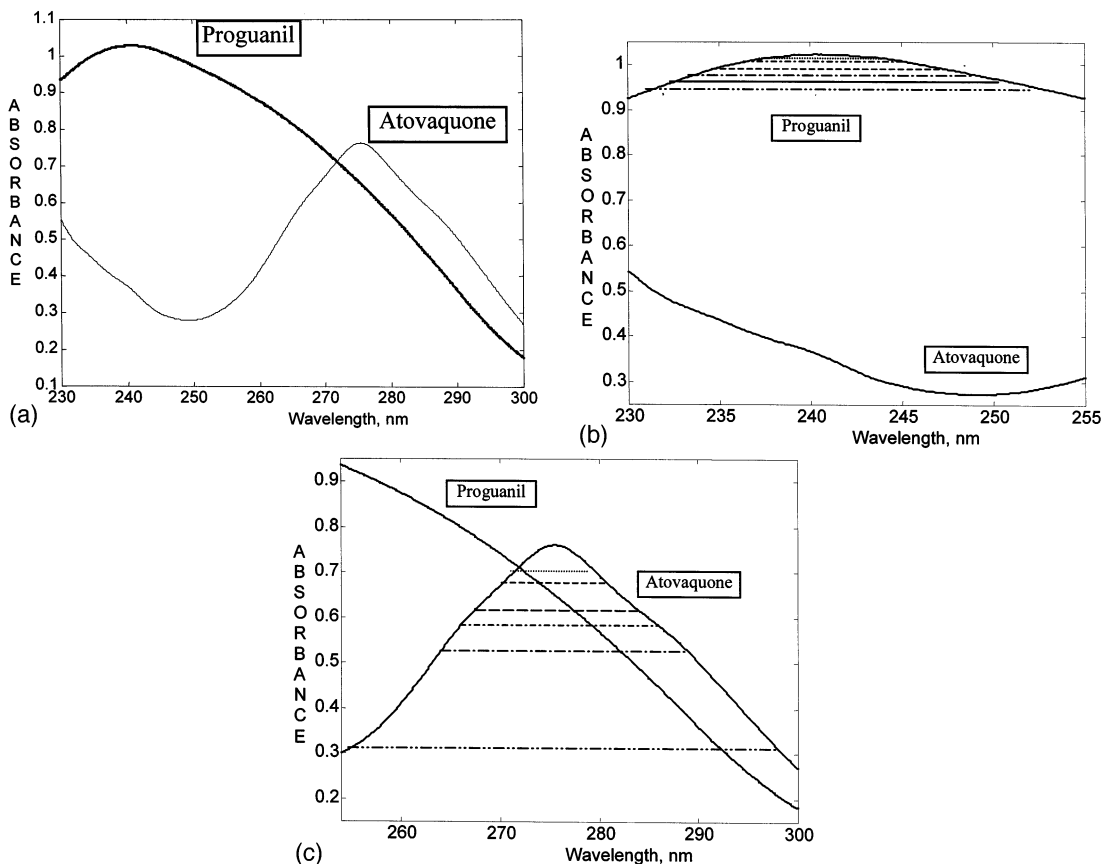


Fig. 2. (a) Absorption spectra of atovaquone (27.58 $\mu\text{mol/l}$) and proguanil (68.57 $\mu\text{mol/l}$). (b) Absorption spectra of atovaquone (27.58 $\mu\text{mol/l}$) and proguanil (68.57 $\mu\text{mol/l}$). Selection of wavelength pairs for proguanil as the interferent: 237.2/243.9; 236.3/245.0; 234.6/247.1; 233.3/248.9; 232.3/250.3; 231.0/252.1 nm. (c) Absorption spectra of atovaquone (27.58 $\mu\text{mol/l}$) and proguanil (68.57 $\mu\text{mol/l}$). Selection of wavelength pairs for atovaquone as the interferent: 271.4/279.3; 270.1/280.3; 267.4/283.9; 266.0/285.9; 263.9/288.7; 254.6/297.8 nm.

Table 8
Results for mixture 5 from additions of atovaquone^a

λ_1/nm ($\bar{M} \pm s_M$) [*]	λ_2/nm ($\bar{M} \pm s_M$) [*]	Atovaquone found (C_H)		Proguanil hydrochloride found (from A_H)	
		$\mu\text{mol/l}$	%	$\mu\text{mol/l}$	%
252.1 (10 189 \pm 79)	231.0 (19 194 \pm 1344)	12.95 \pm 1.97	94.5 \pm 14.4	7.66 \pm 1.48	111.8 \pm 21.5
250.3 (9867 \pm 86)	232.3 (17 881 \pm 972)	12.99 \pm 1.60	94.8 \pm 11.7	7.59 \pm 1.16	110.7 \pm 16.9
248.9 (9823 \pm 86)	233.3 (17 147 \pm 775)	13.08 \pm 1.33	95.4 \pm 9.7	7.51 \pm 0.95	109.5 \pm 13.8
247.1 (9982 \pm 87)	234.6 (16 309 \pm 561)	13.13 \pm 1.11	95.8 \pm 8.1	7.45 \pm 0.81	108.6 \pm 11.8
245.0 (10 456 \pm 88)	236.3 (15 204 \pm 381)	12.99 \pm 0.94	94.8 \pm 6.8	7.56 \pm 0.68	110.3 \pm 9.9
243.9 (10 877 \pm 99)	237.2 (14 666 \pm 315)	13.00 \pm 0.81	94.8 \pm 5.9	7.56 \pm 0.64	110.3 \pm 9.3
λ_{max} : 240.6/275.2 nm		13.79 \pm 0.06	100.6 \pm 0.5	7.05 \pm 0.26	102.8 \pm 3.8

^a Atovaquone (analyte): 13.71 $\mu\text{mol/l}$; proguanil hydrochloride (interferent): 6.86 $\mu\text{mol/l}$.

* \bar{M} , mean slope of the addition line; s_M , standard deviation of the slope.

Table 9
Results from additions of atovaquone to Malarone^a

$\lambda_1/\text{nm} (\bar{M} \pm s_M)^*$	$\lambda_2/\text{nm} (\bar{M} \pm s_M)^*$	Atovaquone found (C_H)		Proguanil hydrochloride found (from A_H)	
		mg/tablet	%	mg/tablet	%
252.1 (10 104 ± 187)	231.0 (19 341 ± 1235)	198.6 ± 32.2	79.4 ± 12.9	129.8 ± 17.6	129.8 ± 17.6
250.3 (9805 ± 204)	232.3 (17 971 ± 948)	205.9 ± 27.6	82.3 ± 11.1	123.4 ± 14.2	123.4 ± 14.2
248.9 (9763 ± 213)	233.3 (17 200 ± 764)	210.6 ± 23.4	84.3 ± 9.3	119.9 ± 11.6	119.9 ± 11.6
247.1 (9925 ± 209)	234.6 (16 343 ± 584)	214.0 ± 19.0	85.6 ± 7.6	117.6 ± 9.1	117.6 ± 9.1
245.0 (10 409 ± 230)	236.3 (15 192 ± 441)	217.9 ± 15.6	87.1 ± 6.3	115.4 ± 7.8	115.4 ± 7.8
243.9 (10 832 ± 230)	237.2 (14 630 ± 376)	219.6 ± 13.7	87.9 ± 5.5	114.6 ± 7.4	114.6 ± 7.4
λ_{max} : 240.6/275.2 nm		248.8 ± 1.9	99.5 ± 0.8	95.9 ± 2.7	95.9 ± 2.7

^a Atovaquone (analyte): 250 mg/tablet; proguanil hydrochloride (interferent): 100 mg/tablet.

* \bar{M} , mean slope of the addition line; s_M , standard deviation of the slope.

Table 10
Results for mixture 6 from additions of proguanil hydrochloride^a

$\lambda_1/\text{nm} (\bar{M} \pm s_M)^*$	$\lambda_2/\text{nm} (\bar{M} \pm s_M)^*$	Proguanil hydrochloride found (C_H)		Atovaquone found (from A_H)	
		$\mu\text{mol/l}$	%	$\mu\text{mol/l}$	%
297.8 (3060 ± 83)	254.6 (13 547 ± 108)	13.65 ± 0.11	99.6 ± 0.8	5.75 ± 0.09	104.3 ± 1.6
288.7 (5608 ± 68)	263.9 (12 032 ± 86)	13.21 ± 0.14	96.3 ± 1.0	5.90 ± 0.09	106.9 ± 1.6
285.9 (6436 ± 61)	266.0 (11 622 ± 71)	13.21 ± 0.21	96.3 ± 1.5	5.86 ± 0.10	106.2 ± 1.9
283.9 (7022 ± 72)	267.4 (11 332 ± 92)	13.05 ± 0.20	95.2 ± 1.5	5.92 ± 0.12	107.3 ± 2.2
280.3 (8079 ± 61)	270.1 (10 750 ± 88)	12.06 ± 0.30	87.9 ± 2.2	6.32 ± 0.11	114.6 ± 2.1
279.3 (8363 ± 68)	271.4 (10 441 ± 96)	12.42 ± 0.28	90.6 ± 2.0	6.12 ± 0.11	110.9 ± 2.0
λ_{max} : 240.6/275.2 nm		13.81 ± 0.10	100.7 ± 0.7	5.57 ± 0.05	101.0 ± 1.0

^a Proguanil hydrochloride (analyte): 13.71 $\mu\text{mol/l}$; atovaquone (interferent): 5.52 $\mu\text{mol/l}$.

* \bar{M} , mean slope of the addition line; s_M , standard deviation of the slope.

precision. In that wavelength region, a high influence of the methanol content on the spectra of both atovaquone and proguanil was experienced. Therefore, these deviations might be related to small differences in the methanol concentration in the solution. The concentrations of proguanil hydrochloride (the interferent) obtained from the absorbance at the H-point are about 10% higher than the expected value. Precision shows the same tendency than for the analyte. The results of the λ_{max} -method are both more precise and more accurate. The same problem is experienced in the analysis of Malarone tablets (Table 9) for which no acceptable results are obtained with the HPSAM.

Tables 10–12 show the results for proguanil hydrochloride considered as the analyte in the

synthetic mixtures and in the Malarone tablets, respectively. Mixture 7 (Table 11) is very similar to the Malarone solutions measured (Table 12). In both samples, the contribution of the interferent (atovaquone) in the wavelength range of the spectrum applicable for the HPSAM, is much larger than that of the analyte. The wavelength pair resulting in the largest difference ($M(\lambda_1) - M(\lambda_2)$) is the pair 297.8/254.6 nm which however does not lead to the most accurate results. This might be due to the very low analyte absorbance in the sample at 297.8 nm. Accurate results are obtained, both for the synthetic mixture as well as for the Malarone tablets, at the wavelength pair 285.9/266 nm which still leads to two addition lines with a considerable difference in slope. When the contribution of proguanil increases, as is the case in mixture 6

(Table 10), where in the applicable wavelength range its contribution in the spectrum is comparable to that of the interferent, accurate and precise results for the analyte are obtained at the wavelength pair 297.8/254.6 nm.

From the above experiments, it follows that the selection of the wavelength pairs to be used in the HPSAM is not always evident. Therefore, the GHPSAM is evaluated on the same mixtures in the next section. This method does not require the spectrum of the interferent to be known since the location of the interval of the unknown interferent (required for the method to be applicable) is derived from the second derivative spectra of the analyte and the sample.

4.2. GHPSAM

4.2.1. Results based on the first approach to locate the linear range of the interferent (see Appendix A)

To locate the linear spectral interval for the interferent, the ratio between the second derivative of the absorbance of the sample, $[A_s(\lambda_j)]\ddot{E}$, and the second derivative of the molar absorption coefficient of the analyte, $[\varepsilon_x]\ddot{E}$, versus the wavelength, λ_j , was plotted for each replicate of the mixtures evaluated. To obtain these plots, the spectral data were taken with intervals of 1 nm to avoid too high noise. All spectral data recorded

Table 11
Results for mixture 7 from additions of proguanil hydrochloride^a

λ_1/nm ($\bar{M} \pm s_M$) [*]	λ_2/nm ($\bar{M} \pm s_M$) [*]	Proguanil hydrochloride found (C_H)		Atovaquone found (from A_H)	
		$\mu\text{mol/l}$	%	$\mu\text{mol/l}$	%
297.8 (3060 ± 102)	254.6 (13 537 ± 125)	6.56 ± 0.14	95.7 ± 2.1	14.62 ± 0.21	106.6 ± 1.6
288.7 (5681 ± 114)	263.9 (12 046 ± 126)	6.37 ± 0.19	92.8 ± 2.7	14.32 ± 0.14	104.5 ± 1.1
285.9 (6548 ± 117)	266.0 (11 636 ± 121)	6.85 ± 0.17	99.9 ± 2.5	13.99 ± 0.14	102.1 ± 1.0
283.9 (7135 ± 114)	267.4 (11 350 ± 132)	6.69 ± 0.16	97.5 ± 2.4	14.09 ± 0.10	102.8 ± 0.7
280.3 (8151 ± 130)	270.1 (10 757 ± 134)	4.06 ± 0.37	59.2 ± 5.4	15.25 ± 0.08	111.2 ± 0.6
279.3 (8434 ± 113)	271.4 (10 449 ± 127)	5.26 ± 0.44	76.7 ± 6.5	14.67 ± 0.11	107.0 ± 0.1
λ_{max} : 240.6/275.2 nm		7.29 ± 0.22	106.3 ± 3.2	13.85 ± 0.05	101.0 ± 0.4

^a Proguanil hydrochloride (analyte): 6.86 $\mu\text{mol/l}$; Atovaquone (interferent): 13.71 $\mu\text{mol/l}$.

* \bar{M} , mean slope of the addition line; s_M , standard deviation of the slope.

Table 12
Results from additions of proguanil hydrochloride to Malarone^a

λ_1/nm ($\bar{M} \pm s_M$) [*]	λ_2/nm ($\bar{M} \pm s_M$) [*]	Proguanil hydrochloride found (C_H)		Atovaquone found (from A_H)	
		mg/tablet	%	mg/tablet	%
297.8 (2986 ± 72)	254.6 (13 487 ± 67)	92.8 ± 0.8	92.8 ± 0.8	264.0 ± 3.0	105.6 ± 1.2
288.7 (5632 ± 57)	263.9 (11 983 ± 68)	93.1 ± 2.7	93.1 ± 2.7	256.2 ± 1.6	102.5 ± 0.6
285.9 (6496 ± 62)	266.0 (11 578 ± 66)	99.4 ± 1.8	99.4 ± 1.8	250.9 ± 1.7	100.4 ± 0.7
283.9 (7084 ± 65)	267.4 (11 285 ± 68)	98.4 ± 2.4	98.4 ± 2.4	251.8 ± 1.4	100.7 ± 0.6
280.3 (8101 ± 67)	270.1 (10 696 ± 69)	60.9 ± 1.9	60.9 ± 1.9	272.4 ± 1.5	109.0 ± 0.6
279.3 (8379 ± 68)	271.4 (10 391 ± 72)	77.5 ± 3.2	77.5 ± 3.2	262.4 ± 1.6	105.0 ± 0.6
λ_{max} : 240.6/275.2 nm		102.4 ± 2.7	102.4 ± 2.7	250.4 ± 2.1	100.2 ± 0.8

^a Proguanil hydrochloride (analyte): 100 mg/tablet; atovaquone (interferent): 250 mg/tablet.

* \bar{M} , mean slope of the addition line; s_M , standard deviation of the slope.

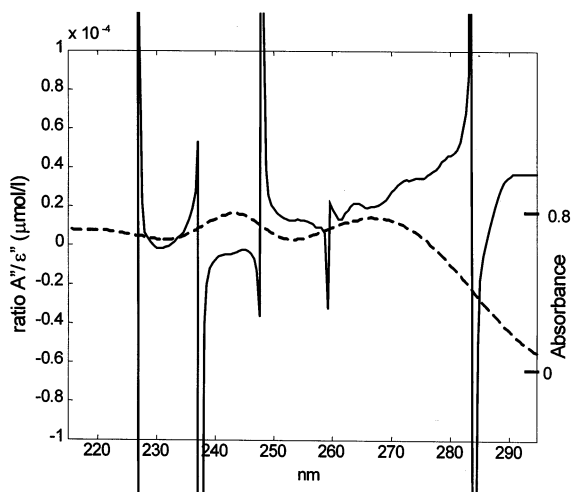


Fig. 3. Plot of $[A_s(\lambda_j)]''/[\varepsilon_X(\lambda_j)]''$ for mixture 1 (analyte: phenazone, interferent: caffeine). The dotted line is the spectrum of phenazone (84.8 $\mu\text{mol/l}$).

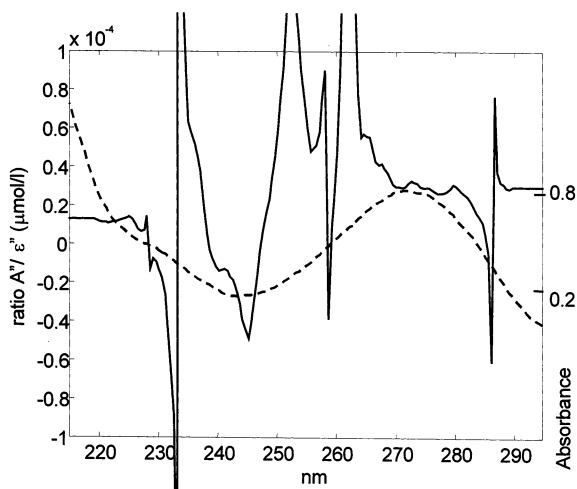


Fig. 4. Plot of $[A_s(\lambda_j)]''/[\varepsilon_X(\lambda_j)]''$ for mixture 3 (analyte: caffeine, interferent: phenazone). The dotted line is the spectrum of caffeine (82.9 $\mu\text{mol/l}$).

with a stepwidth of 0.1 nm were used for the calculation of the third wavelength and therefore also for the calculation of the concentration.

Besides the wavelength pair, λ_1 and λ_2 , and the concentration found, the following tables also contain the mean values for the slopes of the standard addition lines and the mean of the K -values obtained from the maximization of Eq. (11) (Ap-

pendix A). The third wavelength, λ_k , is not indicated in the tables since for each replicate this wavelength was not always the same.

4.2.1.1. Phenazone as the analyte. Fig. 3 shows the plot of $[A_s(\lambda_j)]''/[\varepsilon_X(\lambda_j)]''$ versus λ_j for one of the replicates of mixture 1 in which caffeine is considered the interferent. In this figure, the absorption spectrum for the analyte phenazone is also given. Two rather small intervals in which $[A_s(\lambda_j)]''/[\varepsilon_X(\lambda_j)]''$ is constant, and consequently linear behaviour of the interferent is to be expected, can be identified: the first is located at [240, 245] nm, the second at [250, 258] nm. However since both intervals correspond to different values of $[A_s(\lambda_j)]''/[\varepsilon_X(\lambda_j)]''$, the estimated analyte concentrations from measurements made in both intervals are expected to differ. Measurements in the first interval yield a negative concentration for phenazone (-5.9 ± 0.9 $\mu\text{mol/l}$) while for the second interval, the phenazone concentration is highly overestimated (19.5 ± 0.4 $\mu\text{mol/l}$). This corroborates the conclusion made by Campins Falco that larger errors are to be expected when the contribution of the interferent in the spectrum of the mixture is larger than for the analyte (as is the case in mixture 1). Better, but still unacceptable results are obtained for phenazone in mixture 2, in which the contribution of caffeine (the interferent) in the spectrum of the mixture is lower than for phenazone. This might be attributed to the fact that in both intervals, in which the spectral behaviour of the interferent is expected to be linear, the analyte absorbance is almost linear, too. This follows from the relatively small \bar{K} -values (between 200 and 360) and is confirmed by an inspection of the spectrum of phenazone in Fig. 3. Since the GHPSAM failed for the determination of phenazone in the synthetic mixtures, the poor results obtained for the pharmaceutical formulation Parmentier (not shown here) were to be expected.

4.2.1.2. Caffeine as the analyte. Inspection of Fig. 4 in which the ratio $[A_s(\lambda_j)]''/[\varepsilon_X(\lambda_j)]''$ is plotted as a function of the wavelength for mixture 3 reveals a constant ratio at the very low end of the wavelength range, namely [215, 225] nm. Another wavelength interval in which linear spectral behaviour

Table 13

Results of the GHPSAM (1st approach)^a from additions of caffeine (mixtures 3 and 4)

λ_1/nm	λ_2/nm	$\bar{M}(\lambda_1)^b$	$\bar{M}(\lambda_k)^b$	$\bar{M}(\lambda_2)^b$	\bar{K}	Caffeine found (C_H) (mean \pm S.D.)	
						$\mu\text{mol/l}$	%
Caffeine (analyte): 16.58 $\mu\text{mol/l}$; phenazone (interferent): 16.96 $\mu\text{mol/l}$							
268.0	276.0	8767	9269	8862	454	26.57 \pm 1.35	160 \pm 8
215.0	225.0	13 917	8181	5950	1553	16.21 \pm 0.28	97.8 \pm 1.7
λ_{max} : 242.8/272.2 nm						16.56 \pm 0.11	99.9 \pm 0.7
Caffeine (analyte): 20.93 $\mu\text{mol/l}$; phenazone (interferent): 42.72 $\mu\text{mol/l}$							
215.0	222.0	14 113	9535	7116	664	22.86 \pm 1.31	109.4 \pm 6.2
215.0	223.0	14 113	8944	6639	935	21.21 \pm 0.73	101.3 \pm 3.3
215.0	224.0	14 113	8381	6281	1235	19.89 \pm 0.52	95.0 \pm 2.5
215.0	225.0	14 113	8173	6018	1555	18.99 \pm 0.46	90.7 \pm 2.2
λ_{max} : 242.8/272.2 nm						21.13 \pm 0.19	100.9 \pm 0.9

^a See Appendix A.^b $\bar{M}(\lambda_j)$, mean slope of the addition line measured at λ_j .

of phenazone (the interferent) is expected is found at [268, 276] nm. Since the value of $[A_s(\lambda_j)]''/[e_X(\lambda_j)]''$ in both intervals again is obviously different, different concentrations for caffeine estimated from measurements in both are to be expected. That this is indeed the case follows from Table 13 (upper part) in which the results of the GHPSAM are given. The poor results obtained in the [268, 276] nm interval can again be attributed to the fact that in this interval the spectral behaviour of caffeine is almost linear as follows from the relatively low \bar{K} -value and an inspection of the caffeine spectrum also shown in Fig. 4. Acceptable results for caffeine in terms of accuracy and precision are obtained when measurements are performed in the [215, 225] nm interval. They are almost comparable with those obtained from the λ_{max} -method. When the contribution of phenazone (the interferent) in the spectrum of the mixture increases, as is the case with mixture 4 (lower part of Table 13), the results get worse. They differ by about 10% from the results obtained with the λ_{max} -method, which yields very good results. Notice that restricting the selected wavelength interval by 1 or 2 nm by taking λ_2 at 224 and 223 nm, respectively, considerably improves the results. This points to the importance of the correct selection of the wavelength interval

to be used which is not always obvious from the plot. Since mixture 4 is a simulation of the pharmaceutical formulation Parmentier, similar results were to be expected and were indeed obtained for the determination of caffeine in the formulation (not shown here).

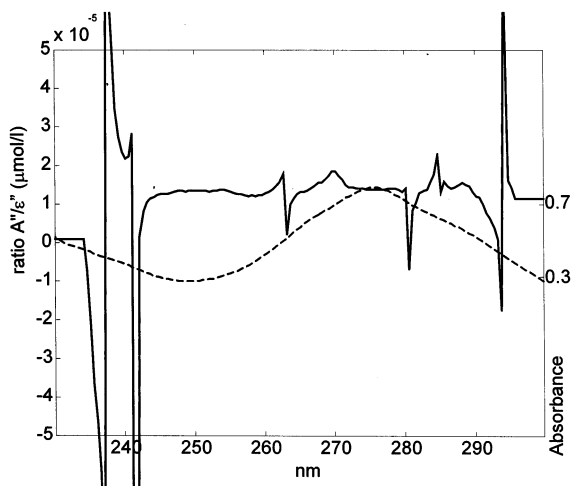


Fig. 5. Plot of $[A_s(\lambda_j)]''/[e_X(\lambda_j)]''$ for mixture 5 (analyte: atovaquone, interferent: proguanil). The dotted line is the spectrum of atovaquone (27.58 $\mu\text{mol/l}$).

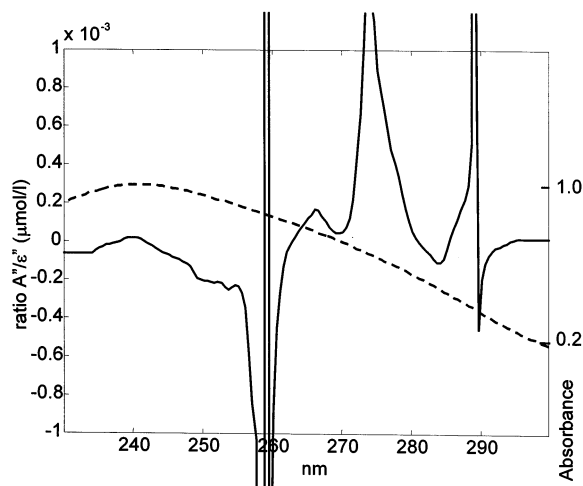


Fig. 6. Plot of $[A_s(\lambda_j)]E''/[ε_X(\lambda_j)]E''$ for mixture 6 (analyte: proguanil, interferent: atovaquone). The dotted line is the spectrum of proguanil (68.57 $\mu\text{mol/l}$).

4.2.1.3. Atovaquone as the analyte. The plot of $[A_s(\lambda_j)]E''/[ε_X(\lambda_j)]E''$ versus λ_j for mixture 5, where proguanil is considered the interferent, is given in Fig. 5. Two wavelength ranges for which $[A_s(\lambda_j)]E''/[ε_X(\lambda_j)]E''$ can be considered constant are observed. They are located at [245, 260] nm and [272, 278] nm. The spectrum of atovaquone (the analyte), which is also indicated in Fig. 5, shows a minimum in the first and a maximum in the second interval selected. This excludes a linear spectral behaviour of the analyte in these intervals. The underestimation of the concentration of atovaquone that resulted from the wavelength interval [245, 260] nm can be seen from Table 14. Better results at least in terms of accuracy are observed for the interval [272, 278] nm. The standard deviation however is 10 times higher than for the λ_{max} -method. The high \bar{K} -values confirm that the analyte does not show linear spectral behaviour. For the addition of atovaquone to solutions of Malarone tablets (not shown here), the first wavelength interval again underestimates the concentration while the interval [272, 278] nm yields an accurate result. As for the simulation, the precision is not acceptable.

4.2.1.4. Proguanil hydrochloride as the analyte. In Fig. 6, which shows the plot of $[A_s(\lambda_j)]E''/$

$[ε_X(\lambda_j)]E''$ versus λ_j for mixture 6, with proguanil hydrochloride considered as the analyte, no wavelength range for which $[A_s(\lambda_j)]E''/[ε_X(\lambda_j)]E''$ is constant can be observed. For an explanation, the spectra of the original solutions given in Fig. 2a are taken into consideration. It can easily be seen that the linear range of atovaquone (the interferent) between 255 and 275 nm falls together with a linear part in the spectrum of proguanil (the analyte) which ranges from 245 to 290 nm. This means that the two requirements of the GHP-SAM, linearity of the interferent and non-linearity of the analyte, cannot be fulfilled. Therefore the GHP-SAM is not applicable to the determination of proguanil hydrochloride in Malarone in which moreover the interferent atovaquone has the largest contribution in the spectrum.

The GHP-SAM has been proposed for analyte determinations in unknown samples. However, as follows from the results presented, it is not evident to locate the linear spectral interval of the interferent by considering $[A_s(\lambda_j)]E''/[ε_X(\lambda_j)]E''$ as a function of the wavelength. This was also recognized by Verdu Andres et al. [6] who proposed an improvement to find the linear intervals. Therefore this second approach was also evaluated here. From the results of the first approach for the location of the linear range of the interferent, it was concluded that the best results are obtained if the analyte has a higher contribution to the spectrum than the interferent. Therefore, only those solutions with the higher analyte concentrations were considered in the evaluation of the second approach.

4.2.2. Results based on the second approach to locate the linear range of the interferent (see Appendix A)

For the evaluation of this second approach, linear regression was repeatedly applied over the whole spectrum considering wavelength intervals between 10 and 40 nm. Linearity for larger wavelength ranges was not expected. The regression lines were considered as linear if r^2 was larger than 0.9999 for the first derivative data and larger than 0.999 for the second derivative data. Linearity in a certain wavelength interval is confirmed if the slopes obtained with first and second derivative data do not differ by more than 5%.

Table 14
Results of the GHPSAM (1st approach)^a from additions of atovaquone (mixture 5)

λ_1/nm	λ_2/nm	$\bar{M}(\lambda_1)^b$	$\bar{M}(\lambda_k)^b$	$\bar{M}(\lambda_2)^b$	\bar{K}	Atovaquone found (C_H) (mean \pm S.D.)	
						$\mu\text{mol/l}$	%
Atovaquone (analyte): 13.71 $\mu\text{mol/l}$; proguanil hydrochloride (interferent): 6.86 $\mu\text{mol/l}$							
245.0	260.0	10 456	10 329	14 897	2381	13.00 \pm 0.21	94.9 \pm 1.5
272.0	278.0	25 762	27 398	26 447	1275	14.09 \pm 0.70	102.8 \pm 5.1
λ_{max} : 240.6/275.2 nm						13.79 \pm 0.06	100.6 \pm 0.5

^a See Appendix A.

^b $\bar{M}(\lambda_j)$, mean slope of the addition line measured at λ_j .

4.2.2.1. Phenazone as the analyte. With the criteria specified above, no linear range could be identified. Therefore, the method is not applicable with phenazone as the analyte and caffeine as the interferent. This confirms the results obtained with the first approach.

4.2.2.2. Caffeine as the analyte. For each replicate of mixture 3, the criteria were fulfilled by 13 or 14 wavelength intervals. As in the first approach, linearity of the interferent (phenazone) was found at the low end of the wavelength range. The largest linear range that can be detected is the interval [215, 228] nm. In the linear regression, no r^2 -value was lower than 0.9998 for the second derivative, while the difference in slopes between first and second derivative data ranged from 3.2 to 3.9%. An average of 15.65 ± 0.38 $\mu\text{mol/l}$ for the concentration of caffeine corresponding to $94.4 \pm 2.3\%$ is obtained for all replicates based on this largest common wavelength pair (Table 15). Compared to the first approach, this result is both less accurate and less precise. This might be due to the selection of the largest interval that fulfilled the conditions. It followed already from the first approach that the best result is not necessarily obtained with the largest possible linear interval. Consideration of smaller wavelength intervals that fulfill the requirements for linearity shows that the best results—better than for the largest wavelength interval—are obtained for those intervals that have the lowest difference between the slopes of the regression lines obtained with first and second derivative data.

4.2.2.3. Atovaquone as the analyte. Up to 484 intervals per replicate fulfill the requirements for linearity of the interferent (proguanil) specified above. For some of the replicates, the largest linear spectral interval was found to be 40 nm while for others it was 31 nm. As the linear intervals do not completely coincide for all replicates, the largest wavelength interval that is common to all replicates, namely [258, 286] nm was selected. For this interval, a concentration of 13.80 ± 0.12 $\mu\text{mol/l}$ was found for atovaquone, corresponding to $100.7 \pm 0.9\%$. As shown in Table 16, this is comparable in terms of accuracy and precision to the good result of the λ_{max} -method. The difference of the slopes of the regression lines obtained with first and second derivative data ranged between 1.8 and 2.6% for the different replicates.

4.2.2.4. Proguanil hydrochloride as the analyte. As was to be expected from the previous results, no wavelength interval could be identified where the interferent shows a linear behaviour whereas the analyte absorbance is non-linear.

5. Conclusion

The H-point standard additions methods were evaluated for the UV-analysis of mixtures containing two compounds with highly overlapping spectra. In general, these methods do not perform better than the λ_{max} -method.

Table 15
Results of the GHPSAM (2nd approach)^a from additions of caffeine (mixture 3)

λ_1/nm	λ_2/nm	$\bar{M}(\lambda_1)^b$	$\bar{M}(\lambda_k)^b$	$\bar{M}(\lambda_2)^b$	\bar{K}	Caffeine found (C_H) (mean \pm S.D.)	
						$\mu\text{mol/l}$	%
Caffeine (analyte): 16.58 $\mu\text{mol/l}$; phenazone (interferent): 16.96 $\mu\text{mol/l}$							
215.0	228.0	13 917	7366	5369	2343	15.65 ± 0.38	94.4 ± 2.3
λ_{max} : 242.8/272.2 nm						16.56 ± 0.11	99.9 ± 0.7

^a See Appendix A.

^b $\bar{M}(\lambda_j)$, mean slope of the addition line measured at λ_j .

Table 16
Results of the GHPSAM (2nd approach)^a from additions of atovaquone (mixture 5)

λ_1/nm	λ_2/nm	$\bar{M}(\lambda_1)^b$	$\bar{M}(\lambda_k)^b$	$\bar{M}(\lambda_2)^b$	\bar{K}	Atovaquone found (C_H) (mean \pm S.D.)	
						$\mu\text{mol/l}$	%
Atovaquone (analyte): 13.71 $\mu\text{mol/l}$; proguanil hydrochloride (interferent): 6.86 $\mu\text{mol/l}$							
258	286	13 134	27 329	20 898	1422	13.80 \pm 0.12	100.7 \pm 0.9
λ_{max} : 240.6/275.2 nm						13.79 \pm 0.06	100.6 \pm 0.5

^a See Appendix A.

^b $\bar{M}(\lambda_j)$, mean slope of the addition line measured at λ_j .

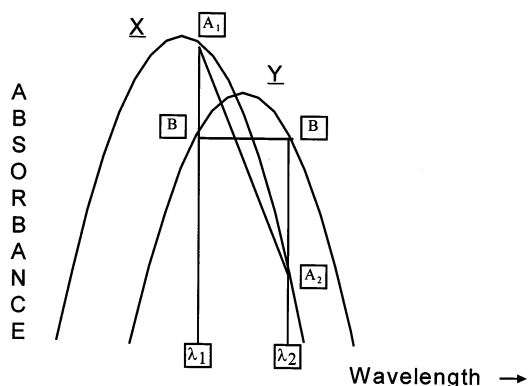


Fig. 7. Absorption spectra of the analyte, X, and the interferent, Y fulfilling the requirements for the HPSAM (see text).

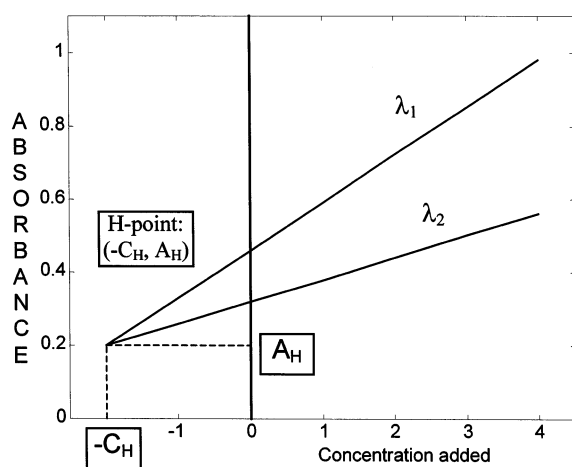


Fig. 8. H-point standard addition lines.

The HPSAM performs generally best when the wavelength pair chosen for measuring the analyte leads to the largest difference between the slopes of the standard addition lines ($M(\lambda_1) - M(\lambda_2)$). This is however no longer the case if at λ_1 or λ_2 the absorbance of the analyte in the sample is very small. Acceptable results can then be obtained only when measurements are performed at two wavelengths where the analyte absorbance is not too small and the difference in slopes of the addition lines is large enough. (The additional requirement that the interferent shows the same absorbance at both wavelength of course has to be fulfilled.) The selection of the appropriate wavelength pairs is therefore not always evident.

In contrast to the HPSAM, the generalized HPSAM (GHPSAM) does not require the spectrum of the interferent to be known and is thus theoretically applicable for the analysis of unknown samples. From the evaluation performed in this work it follows that without a reference solution that contains the analyte as well as the interferent, the selection of the wavelength interval to be used for measuring the analyte is not obvious at all. Moreover in each of the two two-component systems analyzed here, only one of the two compounds could be determined (caffeine in the caffeine/phenazone mixtures and atovaquone in the atovaquone/proguanil mixtures). The GHPSAM failed for the determination of phenazone in the caffeine/phenazone mixtures and for the determination of proguanil in the atovaquone/proguanil mixtures. This is due to the fact that their absorbance also shows an almost linear behaviour in the wavelength interval(s) in which the spectral behaviour of the component considered as the interferent (caffeine and atovaquone, respectively) was found to be linear.

Acknowledgements

The authors thank the European Community Standards, Measurements and Testing research programme for financial support (project SMT4-CT95-2031). They are grateful to A. De Schrijver and K. Decq for technical aid.

Appendix A. Theoretical background of the HPSAM and the GHPSAM

A.1. H-point standard additions method (HPSAM) [1,3]

The method which requires the spectrum of the interferent to be known, is based on measurements of a standard addition line at two wavelengths λ_1 and λ_2 where the interferent Y shows the same absorbance. The absorbance of the analyte X at λ_1 and λ_2 should be different (Fig. 7).

The two standard addition lines intersect at the so-called H-point with co-ordinates $(-C_H, A_H)$,

where C_H is the concentration of the analyte and A_H the analytical signal due to the interferent (Fig. 8).

The addition lines obtained at the wavelengths λ_1 and λ_2 are given by:

$$A(\lambda_1) = B + A_1 + M(\lambda_1) \cdot C_X^i \quad (1)$$

$$A(\lambda_2) = B + A_2 + M(\lambda_2) \cdot C_X^i \quad (2)$$

A_1 and A_2 denote the absorbances of the analyte in the sample at λ_1 and λ_2 , respectively, B is the absorbance of the interferent which is the same at λ_1 and λ_2 , $M(\lambda_1)$ and $M(\lambda_2)$ are the slopes of the addition lines, and C_X^i is the concentration of the analyte added. The addition lines intersect at the H-point, $(-C_H, A_H)$, given by:

$$A_1 + M(\lambda_1) \cdot (-C_H) = A_2 + M(\lambda_2) \cdot (-C_H)$$

This can also be written as:

$$\begin{aligned} -C_H &= \frac{(A_2 - A_1)}{M(\lambda_1) - M(\lambda_2)} \\ &= \frac{C_X^0 \cdot (M(\lambda_2) - M(\lambda_1))}{M(\lambda_1) - M(\lambda_2)} = -C_X^0 \end{aligned} \quad (3)$$

The unknown analyte concentration C_X^0 therefore corresponds to C_H .

The absorbance at the H-point, A_H , corresponds to the absorbance of the interferent since from Eq. (1):

$$\begin{aligned} A(\lambda_1) &= B + A_1 + M(\lambda_1) \cdot (-C_H) \\ &= B + M(\lambda_1) \cdot C_X^0 + M(\lambda_1) \cdot (-C_H) \\ &= B \end{aligned} \quad (4)$$

If required, the concentration of the interferent can then be calculated from a calibration line for the pure interferent at λ_1 (or λ_2).

A.2. Generalized H-point standard additions method (GHPSAM) [5,6]

This method which does not require the spectrum of the interferent to be known is based on measurements of a standard addition line at three wavelengths λ_1, λ_k , and λ_2 with $\lambda_k \in [\lambda_1, \lambda_2]$. The first requirement is that the unknown interferent has to show a linear behaviour between λ_1 and λ_2 . The second restriction for the selection of these wavelengths is related to the analyte, which has to show absorbance values that are not linearly related in the wavelength interval $[\lambda_1, \lambda_2]$ (Fig. 9a). Two

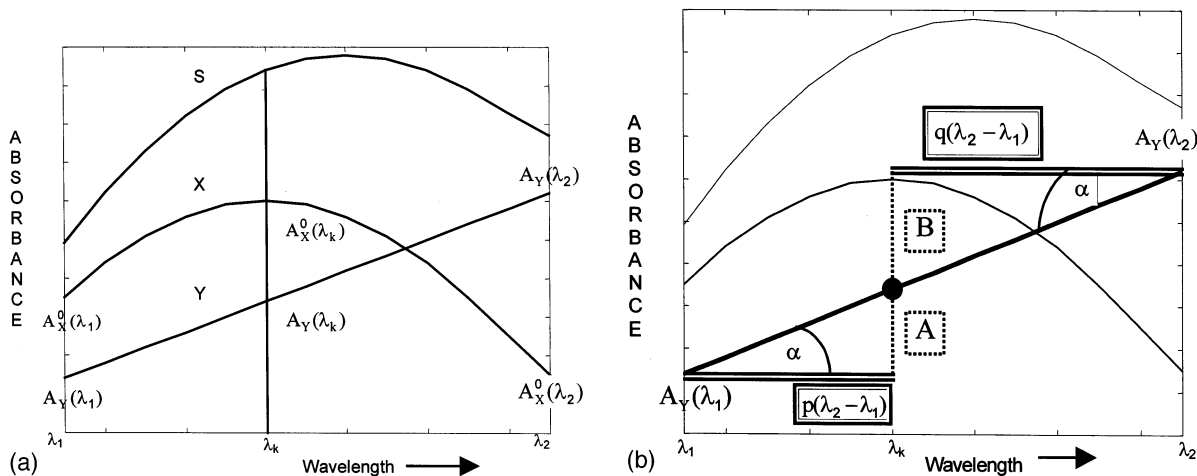


Fig. 9. (a) Conditions for the spectra required in the GHPSAM (X: analyte, Y: interferent, S: sample). (b) Geometrical proof for the equality

$$(A_Y(\lambda_k) - A_Y(\lambda_1))/p = (A_Y(\lambda_k) - A_Y(\lambda_2))/q$$

$$(A = A_Y(\lambda_k) - A_Y(\lambda_1), B = A_Y(\lambda_k) - A_Y(\lambda_2))$$

approaches have been described to locate the linear spectral behaviour for the unknown interferent.

A.2.1. First approach to locate the linear spectral behaviour of the unknown interferent [5]

The straight line that describes the linear spectral behaviour of the interferent between λ_1 and λ_2 is given by:

$$[A_Y(\lambda_j)] = [A_Y(\lambda_1)] + b \cdot \lambda_j \quad \lambda_j \in [\lambda_1, \lambda_2] \quad (5)$$

This line remains the same during the additions of the analyte X . However, the absorbance of the analyte in the same wavelength interval increases with the additions of X :

$$[A_X^i(\lambda_j)] = C_X^i \cdot \varepsilon_X(\lambda_j) \quad (i = 0, 1, \dots, n)$$

where $\varepsilon_X(\lambda_j)$ is the molar absorption coefficient of the analyte at the wavelength λ_j . For $i = 0$, the original sample solution without any additions, the absorbance at λ_j is given by:

$$[A_S(\lambda_j)] = [A_X^0(\lambda_j)] + [A_Y(\lambda_j)] \\ = C_X^0 \cdot \varepsilon_X(\lambda_j) + [A_Y(\lambda_1)] + b \cdot \lambda_j \quad (6)$$

If the interferent shows a linear behaviour in the wavelength interval considered, the second derivative of the sample absorbance with respect to the wavelength should only contain a contribution of the analyte:

$$\frac{d^2[A_S(\lambda_j)]}{d\lambda^2} = \frac{d^2[A_X^0(\lambda_j)]}{d\lambda^2} + \frac{d^2[A_Y(\lambda_j)]}{d\lambda^2} \\ = C_X^0 \cdot \frac{d^2[\varepsilon_X(\lambda_j)]}{d\lambda^2} \\ = C_X^0 \cdot [\varepsilon_X(\lambda_j)]'' = [A_S(\lambda_j)]''$$

This can also be expressed as:

$$\frac{[A_S(\lambda_j)]''}{[\varepsilon_X(\lambda_j)]''} = C_X^0 \quad (7)$$

Therefore, the linear spectral range of the interferent can be found as the region with a constant ratio of the second derivative of the sample with respect to the wavelength and $[\varepsilon_X(\lambda_j)]''$. For all the wavelengths, $[\varepsilon_X(\lambda_j)]''$ is obtained as the slopes of the calibration lines from the second derivative spectra of the analyte solutions. A plot of $[A_S(\lambda_j)]'' /$

$[\varepsilon_X(\lambda_j)]''$ versus λ_j allows to locate the wavelength interval in which the ratio is constant and consequently the interferent shows a linear behaviour. Moreover as follows from Eq. (7) from the constant ratio an estimate of C_X^0 can be obtained. However, to estimate the analyte concentration more accurately, the GHPSAM described later has to be applied.

A.2.2. Second approach to locate the linear spectral behaviour of the unknown interferent

Recently, a second approach for the selection of the linear range of the unknown interferent based both on first and second-derivative data has been proposed [6]. The absorbance of a reference analyte solution with concentration C_X^R is:

$$[A_X^R(\lambda_j)] = C_X^R \cdot [\varepsilon_X(\lambda_j)]$$

The first derivative is $[A_X^R(\lambda_j)]' = C_X^R \cdot [\varepsilon_X(\lambda_j)]'$, and the second derivative $[A_X^R(\lambda_j)]'' = C_X^R \cdot [\varepsilon_X(\lambda_j)]''$.

If the spectral behaviour of the unknown interferent Y in the wavelength interval $[\lambda_1, \lambda_2]$ is linear, then Eq. (5) applies:

$$[A_Y(\lambda_j)] = [A_Y(\lambda_1)] + b \cdot \lambda_j$$

The first derivative is then $[A_Y(\lambda_j)]' = b$, while the second derivative is $[A_Y(\lambda_j)]'' = 0$.

The absorbance of the sample is given by Eq. (6) with first and second derivatives equal to $[A_S(\lambda_j)]' = C_X^0 \cdot [\varepsilon_X(\lambda_j)]' + b$ and $[A_S(\lambda_j)]'' = C_X^0 \cdot [\varepsilon_X(\lambda_j)]''$, respectively.

The linear wavelength intervals of the interferent can now be obtained from the first derivative data:

$$[A_S(\lambda_j)]' - [A_X^R(\lambda_j)]' = b + (C_X^0 - C_X^R) \cdot [\varepsilon_X(\lambda_j)]' \\ = b + \frac{(C_X^0 - C_X^R)}{C_X^R} \cdot [A_X^R(\lambda_j)]' \quad (8)$$

A plot of the values of the difference between the first derivative of the sample and the first derivative of the reference analyte solution versus the first derivative of the reference solution results in a straight line with intercept b and slope

$$\frac{(C_X^0 - C_X^R)}{C_X^R}$$

In order to better locate the linear spectral wavelength interval for the interferent from the first derivative data, linear regressions are calculated considering different wavelength intervals. Starting with a small wavelength interval $\Delta\lambda = 10$ nm, linear regressions are calculated for both first and second derivative data for the intervals $[\lambda_0; \lambda_0 + \Delta\lambda]$, $[\lambda_0 + 1; \lambda_0 + 1 + \Delta\lambda]$ till the highest wavelength of the spectrum, λ_z , is reached, $[\lambda_z - \Delta\lambda; \lambda_z]$. The same calculations are then repeated considering increasing wavelength intervals (from $\Delta\lambda = 11$ nm to $\Delta\lambda = \lambda_z - \lambda_0$). The results of the regressions are tested for linearity using the correlation coefficient, r , as a criterion: the r^2 value should at least be equal to 0.9999. Linearity in the wavelength interval is confirmed if the slope for the second derivative data is similar to that for the first derivative data:

$$[A_S(\lambda_j)]'' - [A_X^R(\lambda_j)]'' = (C_X^0 - C_X^R) \cdot [\varepsilon_X(\lambda_j)]'' \\ = \frac{(C_X^0 - C_X^R)}{C_X^R} \cdot [A_X^R(\lambda_j)]'' \quad (9)$$

Indeed a plot of the values of the difference between the second derivative of the sample and the second derivative of the reference analyte solution versus the second derivative of the reference solution yields a straight line with intercept 0 and the same slope:

$$\frac{(C_X^0 - C_X^R)}{C_X^R}$$

Therefore, if the two slopes in Eqs. (8) and (9) are the same for a certain wavelength interval, the spectral behaviour of the interferent in this interval can really be considered as linear.

The calculation of the derivatives is based on the procedures by Gorry [11] and Savitzky and Golay [12].

A.2.3. Selection of the third wavelength

After the wavelength interval $[\lambda_1, \lambda_2]$, in which the behaviour of the interferent can be considered linear, has been identified by one of the two approaches discussed, a third wavelength, λ_k , within this interval has to be selected. First, two further parameters are introduced:

$$p = \frac{\lambda_k - \lambda_1}{\lambda_2 - \lambda_1}; \quad q = \frac{\lambda_2 - \lambda_k}{\lambda_2 - \lambda_1}; \quad p + q = 1$$

Since the interferent shows a linear spectral behaviour in the interval $[\lambda_1, \lambda_2]$, it follows that (Fig. 9b):

$$\frac{[A_Y(\lambda_k) - A_Y(\lambda_1)]}{p} = \frac{[A_Y(\lambda_2) - A_Y(\lambda_k)]}{q} \quad (10)$$

In the interval $[\lambda_1, \lambda_2]$, the analyte should not be linearly related at the three selected wavelengths so that:

$$\frac{[A_X(\lambda_k) - A_X(\lambda_1)]}{p} \neq \frac{[A_X(\lambda_2) - A_X(\lambda_k)]}{q}$$

or

$$A_X(\lambda_k) \neq q \cdot A_X(\lambda_1) + p \cdot A_X(\lambda_2)$$

which means that:

$$\varepsilon_X(\lambda_k) \neq q \cdot \varepsilon_X(\lambda_1) + p \cdot \varepsilon_X(\lambda_2)$$

The third wavelength λ_k is selected in such a manner that the K -value is maximized:

$$|q \cdot \varepsilon_X(\lambda_1) + p \cdot \varepsilon_X(\lambda_2) - \varepsilon_X(\lambda_k)| = K \quad (11)$$

A.2.4. Calculation of the sample concentration C_X^0 by the GHPSAM

The standard addition lines at the three wavelengths selected (Fig. 10a) are given by:

$$A_S(\lambda_1) = A_X^0(\lambda_1) + A_Y(\lambda_1) + M(\lambda_1) \cdot C_X^i$$

$$A_S(\lambda_k) = A_X^0(\lambda_k) + A_Y(\lambda_k) + M(\lambda_k) \cdot C_X^i$$

$$A_S(\lambda_2) = A_X^0(\lambda_2) + A_Y(\lambda_2) + M(\lambda_2) \cdot C_X^i$$

The differences of the addition lines between λ_1 and λ_k and between λ_k and λ_2 are used for the calculation of the addition lines using absorbance increments (Fig. 10b). The weighted difference between $A_S(\lambda_k)$ and $A_S(\lambda_1)$ is given by:

$$\Delta A_S(\lambda_1, \lambda_k) = q \cdot [A_S(\lambda_k) - A_S(\lambda_1)] \\ = q \cdot [A_X^0(\lambda_k) - A_X^0(\lambda_1) + A_Y(\lambda_k) \\ - A_Y(\lambda_1) + (M(\lambda_k) - M(\lambda_1)) \cdot C_X^i] \quad (12)$$

whereas the weighted difference between $A_S(\lambda_2)$ and $A_S(\lambda_k)$ is given by:

$$\Delta A_S(\lambda_k, \lambda_2) = p \cdot [A_S(\lambda_2) - A_S(\lambda_k)]$$

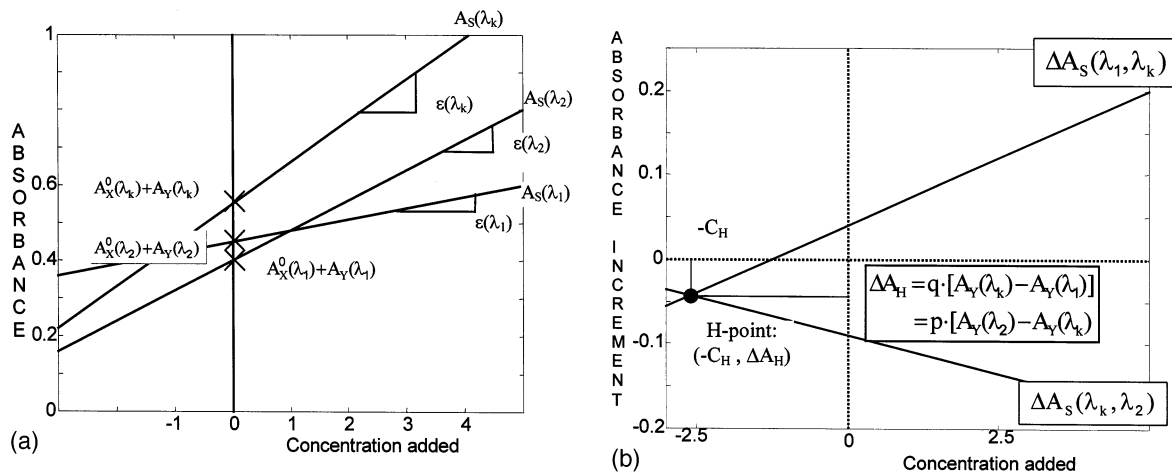


Fig. 10. (a) Standard addition lines at the three wavelengths λ_1 , λ_k and λ_2 . (b) Addition lines using absorbance increments.

$$\begin{aligned}
 &= p \cdot [A_X^0(\lambda_2) - A_X^0(\lambda_k)] \\
 &+ A_Y(\lambda_2) - A_Y(\lambda_k) + (M(\lambda_2) \\
 &- M(\lambda_k)) \cdot C_X^i
 \end{aligned} \quad (13)$$

As linearity is required for the interferent, it follows from Eq. (10) that:

$$q \cdot [A_Y(\lambda_k) - A_Y(\lambda_1)] = p \cdot [A_Y(\lambda_2) - A_Y(\lambda_k)] \quad (14)$$

From the intersection point of the addition lines of the absorbance increments (given by Eqs. (12) and (13)), the H-point ($-C_H$, ΔA_H), the unbiased analyte concentration for the original solution, C_X^0 , can be calculated:

$$\begin{aligned}
 &-C_H \\
 &\left\{ \begin{aligned} &q \cdot [A_X^0(\lambda_k) - A_X^0(\lambda_1) + A_Y(\lambda_k) - A_Y(\lambda_1)] - \\ &p \cdot [A_X^0(\lambda_2) - A_X^0(\lambda_k) + A_Y(\lambda_2) - A_Y(\lambda_k)] \end{aligned} \right\} \\
 &= \frac{p \cdot [M(\lambda_2) - M(\lambda_k)] - q \cdot [M(\lambda_k) - M(\lambda_1)]}{p \cdot [M(\lambda_2) - M(\lambda_k)] - q \cdot [M(\lambda_k) - M(\lambda_1)]} \\
 &= \frac{q \cdot [A_X^0(\lambda_k) - A_X^0(\lambda_1)] - p \cdot [A_X^0(\lambda_2) - A_X^0(\lambda_k)]}{p \cdot [M(\lambda_2) - M(\lambda_k)] - q \cdot [M(\lambda_k) - M(\lambda_1)]} \\
 &= \frac{A_X^0(\lambda_k) - q \cdot A_X^0(\lambda_1) - p \cdot A_X^0(\lambda_2)}{q \cdot M(\lambda_1) + p \cdot M(\lambda_2) - M(\lambda_k)} \\
 &= \frac{C_X^0 \cdot [M(\lambda_k) - q \cdot M(\lambda_1) - p \cdot M(\lambda_2)]}{q \cdot M(\lambda_1) + p \cdot M(\lambda_2) - M(\lambda_k)} \\
 &= -C_X^0
 \end{aligned}$$

The absorbance increment at the intersection

point is given by:

$$\Delta A_H = q \cdot [A_Y(\lambda_k) - A_Y(\lambda_1)] = p \cdot [A_Y(\lambda_2) - A_Y(\lambda_k)]$$

References

- [1] F. Bosch Reig, P. Campins Falco, *Analyst* 113 (1988) 1011–1016.
- [2] M.J. Cardone, *Analyst* 115 (1990) 111–113.
- [3] P. Campins Falco, F. Bosch Reig, *Fresenius J. Anal. Chem.* 338 (1990) 16–21.
- [4] J. Verdu Andres, P. Campins Falco, F. Bosch Reig, *Analyst* 120 (1995) 299–304.
- [5] P. Campins Falco, J. Verdu Andres, F. Bosch Reig, C. Molins Legua, *Anal. Chim. Acta* 302 (1995) 323–333.
- [6] J. Verdu Andres, F. Bosch Reig, P. Campins Falco, *J. Chemom.* 12 (1998) 27–40.
- [7] P. Campins Falco, F. Bosch Reig, R. Herraiez Hernandez, A. Sevillano Cabeza, *Anal. Chim. Acta* 257 (1992) 89–98.
- [8] P. Campins Falco, J. Verdu Andres, F. Bosch Reig, *Analyst* 119 (1994) 2123–2127.
- [9] D.L. Massart, B.G.M. Vandeginste, L.M.C. Buydens, S. de Jong, P.J. Lewi, J. Smeyers-Verbeke, *Handbook of Chemometrics and Qualimetrics: Part A*, Elsevier, Amsterdam, 1997, pp. 109–111.
- [10] J. Smeyers-Verbeke, M.R. Detaevernier, D.L. Massart, *Anal. Chim. Acta* 191 (1986) 181–192.
- [11] P.A. Gorry, *Anal. Chem.* 62 (1990) 570–573.
- [12] A. Savitzky, M.J.E. Golay, *Anal. Chem.* 36 (1964) 1627–1639.